JOURNAL OF MATERIALS SCIENCE 7 (1972) 763–770

Grain-boundary hardening and elastic recovery of micro-indentations

M. BRAUNOVIĆ
Hydro-Quebec Institute of Research, Varennes, Quebec, Canada
C. W. HAWORTH
Department of Metallurgy, University of Sheffield, England

Variation in micro-hardness across a grain boundary, a well-documented effect found in many materials, is here confirmed for zone-refined iron containing 170 at. ppm of tin. Elastic recovery of the impression-diagonal was practically negligible but considerable recovery occurred in the direction of the indentation penetration depth. The latter is different for impressions located at grain boundaries compared with those located at grain interiors, when small loads are applied; however, this difference diminishes with increasing load. Excess hardening at grain boundaries also decreases as the load increases. The results are discussed in terms of the elastic-plastic properties of the material sampled by the impression, and evaluations of some of the parameters are presented. The correlation between grain-boundary hardening and elastic recovery of the impressions is also indicated.

1. Introduction

It is well known that micro-indentation hardness testing is sensitive to inhomogeneities in the microstructure of metallographic specimens. In recent years, this technique was successfully used in studies of the phenomena associated with grain boundaries. It was shown that with a suitable load on a properly prepared specimen surface, the hardness of the material at or in the vicinity of grain boundaries could be compared with the hardness of the grain bulk remote from grain boundaries [1]. Such a comparison revealed that in very pure metals subjected to quenching treatment, an apparent softening occurred at grain boundaries and their immediate vicinity. Addition of certain alloying elements changed this to an apparent increase in hardness at the boundaries. An apparent softening is believed to be associated with the annihilation of quench-produced vacancies at grain boundaries that otherwise contribute to the hardening at locations remote from grain boundaries [2]. The excess hardening observed in the presence of certain solute atoms is believed to be due to solute clustering in the vicinity of the interface as a result of the vacancy gradients which exists there. In the case of pure iron, however, there is no evidence showing softening at grain boundaries, but there is evidence for an increasing excess hardening at grain boundaries with increasing impurity content [3].

It is the aim of this paper to establish whether grain-boundary hardening in iron and iron alloys, as revealed by the use of a micro-indentation technique, is a property of the grain boundaries throughout the bulk of the material that can be understood in terms of a "normal" hardening process (such as precipitation or solid solution) or whether it is an effect intrinsic to micro-indentation hardness testing. For these reasons, and in order to achieve a better understanding of the phenomena occurring at grain boundaries, the analysis of the micro-indentation technique and boundary hardening calls for closer scrutiny.

2. Preliminary consideration of the micro-indentation hardness testing

When a pyramid indenter is pressed into a metal, there is, at first, an elastic deformation front* which moves below the indenter, followed by a curved zone of plastic deformation as the pressure increases. The pressure distribution is not known analytically, but is believed to be roughly uniform, with a high region in the centre and a rapid fall-off near the edge of impression.

All the experimental evidence so far indicates

*Elastic deformation front is visualized as a boundary between the rigid matrix and the zone where the elastic and plastic components of the strain are of comparable magnitude.

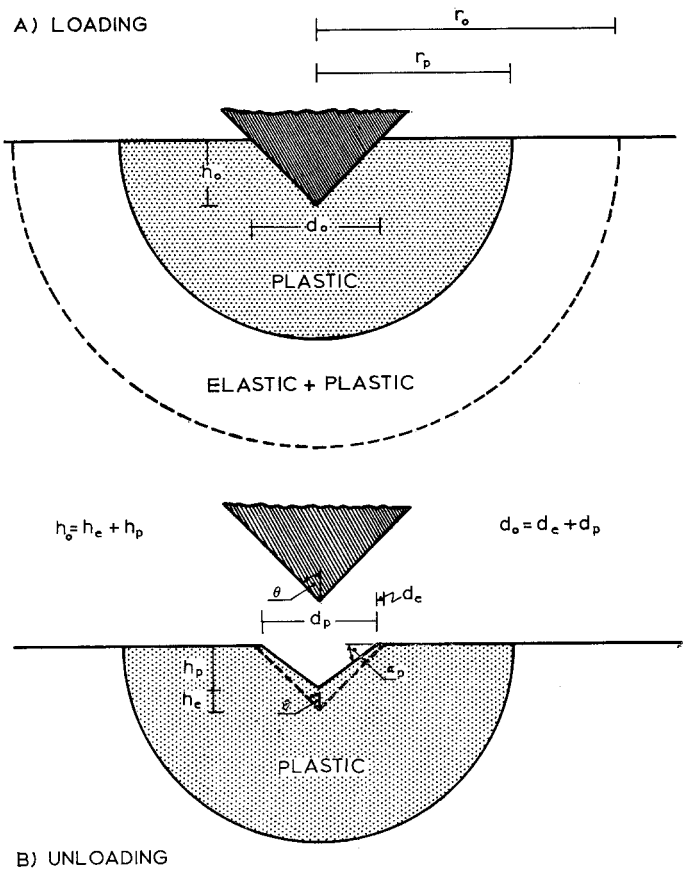

Figure 1 Geometry of the micro-indentation (detailed explanations are given in the text).

that the deformation mechanism which operates during indentation of a metal by a pyramid indenter resembles a uniform radial compression. The boundary between the zone where the material is plastically deformed (work-hardened) and the zone where the material is stressed to the yield point but remains rigid, because of the constraint of the non-plastic matrix, is approximately a hemisphere that is almost unaffected by the detailed shape of the impression itself [4]. Fig. 1a shows the material during loading by an indenter; d_o and h_o are respectively the diagonal and the depth of the indenter penetration; r_o is the radius of the zone of plastic and elastic deformation and r_p is the radius of the zone of plastic deformation.

Upon removal of the indenter, the impression undergoes elastic recovery. The unrecovered residue of the impression is determined by the material plastically deformed with a local hardening gradient forming a "zone of influence" around the impression. This is illustrated in Fig. 1b, which shows the impression after removal of the indenter from a metal; d_p and h_p are respectively the diagonal length and the depth that remain in the material after removal of the indenter, whereas d_e and h_e are respectively the amounts of the contraction that the impression undergoes in the directions of diagonal and depth of penetration. According to a rather simplified model proposed by Mulhearn, the strain pattern in the neighbourhood of an impression is reasonably well expressed by the relationship [5].

$$\epsilon = \frac{4}{3\pi} \cot \frac{\theta}{2} \left(\frac{a/2}{r} \right)^3 \qquad (1)$$

where ϵ is the strain, θ is the angle between the faces of the indenter and equal to 138°, a is the side of an impression, and r is the radius of a hemisphere (zone of influence) across which the material flows radially and uniformly; this radius

is generally assumed to be 10 to 15 times the depth of the indenter penetration [6, 7].

Considerable experimental evidence indicates that elastic recovery of an impression in the direction of the diagonal is practically negligible [5, 6] whereas recovery in the direction of depth of the impression is substantial. This phenomenon can easily be understood in terms of the penetration mechanism of the pyramid indenter, since the heavy specific pressure on the sharp edges of the indenter leads to an irreversible deformation along the diagonals [6]. As a result, the impression that remains in the material is in all circumstances that of the indenter during loading.

In addition, it is of interest to note that a similar phenomenon was observed when a metal was loaded with a conical indenter; no change or practically negligible change was observed in the diameter of the impression, but a considerable decrease was found in its depth [8].

Measurements of elastic recovery by various authors have yielded reasonable consistent values. It was found to be negligible for very soft metals such as lead, 1 to 10% for Al, 5 to 20% for Cu and 10 to 30% for steels [6].

The problem of elastic recovery has been treated theoretically by Love [9] who, using Boussinesq's solution for the deformation of a flat surface by a rigid cone of apical angle θ, derived a relationship for the elastic recovery of the conical indentation in the direction of depth of penetration that is expressed by

$$h_e = \frac{\pi}{2} a \cot \frac{\theta}{2} \tag{2}$$

where h_e is the elastic recovery, a is the radius of the indentation. According to Love's analysis there is a correlation between the apical angle and the mean pressure (p) over the contact region that is given by

$$p = \frac{E \cot \frac{\theta}{2}}{2(1 - \upsilon^2)} \tag{3}$$

where E and υ are Young's modulus and Poisson ratio respectively of the specimen. On the other hand, since the mean pressure and load (L) are related by $p = L/a^2\pi$, the expression for elastic recovery in the direction of depth becomes:

$$h_e = \left(\frac{\pi}{2} \cot \frac{\theta}{2}\right)^{\frac{1}{2}} \cdot \left(\frac{1 - \upsilon^2}{E}\right)^{\frac{1}{2}} \cdot L^{\frac{1}{2}} \tag{4}$$

This expression has been experimentally tested by Stilwell *et al* [8] on various metals, using a tungsten carbide cone. The general trend and the actual values of the elastic recovery, including the recovery of the indenter itself, agree very well with the values predicted by Love's analysis.

It should be noted, however, that Love's analysis has some limitations arising from the assumption that the recovered indentation is bounded by a flat undistributed surface and that it has straight sides. In practice, the free surface is rarely flat owing to the sinking-in or piling-up effects, but these changes in the indentation modes do not seriously affect the elastic analysis [8]. On the other hand, if the sides of the indentation are considerably curved, as in the case of large recoveries, the above analysis cannot be freely applied, because pressure distribution and deformation are not accurately accounted for by this analysis. Consequently this approach cannot be used while dealing with highly elastic materials (polymers, for instance). However, recovery in metals is relatively small [6] and the sides of the indentation are fairly straight. Thus, this analysis is reasonably valid.

3. Experimental procedure

Zone-refined iron containing 170 at. ppm of tin was used in the present work. This material was chosen because an excessive hardening had been detected at grain boundaries; annealing treatments and possible causes for such a hardening are described elsewhere [10]. Annealed specimens for metallographic (interference microscope) and micro-hardness testing were first ground on wet silicon-carbide papers and polished on 6 and 0.25 μm diamond paste. To obtain reliable micro-indentation hardness data, it was necessary to remove the strained surface layer [11] by electropolishing. Details concerning the electropolishing conditions are given elsewhere [3].

The micro-indentation hardness measurements were carried out with a Reichert Micro-Indentation Tester equipped with a diamond-pyramid indenter. The load used in this study was in the range 3.3 to 25 g, corresponding diagonals were from 7 to 24 μm. The time of loading was 5 sec; longer times were used when higher loads were applied, but never longer than 10 sec. Each reported value is the average of ten readings at randomly selected points on either a grain boundary or a grain interior. The grain-boundary indentations were located on the

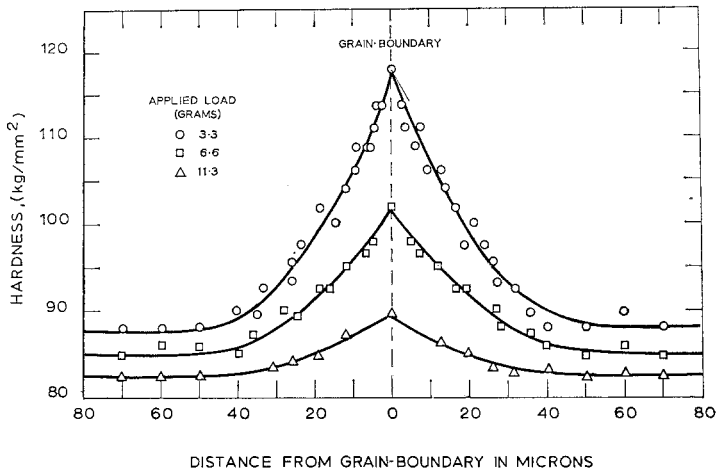

Figure 2 Micro-indentation hardness profiles of a grain boundary in Fe ~ 170 at. ppm of Sn obtained with different loads.

grain boundary ($\pm$ 0.5 μm) and away from the three-grain junction, whereas the grain-interior indentations were taken at the centre of the grain.

In order to minimize the error due to lack of contrast, all measurements were performed using polarization contrast; the error in measuring the indentation diagonal was estimated to be $\pm$ 3%.

4. Results

4.1. Grain-boundary hardening

The results of the measurements using different loads are shown in Figs. 2 and 3. Hardness-distance profiles for some of the loads applied on the indenter are seen in Fig. 2, whilst the dependence of the peak hardness increment ($\Delta H/H_g$) as a function of indenting load is shown in Fig. 3.

It is evident from Fig. 2 that the magnitude of hardening at the grain boundaries and at any given position relative to the grain boundary decreases with increasing indenting load, whilst the extent of the hardness region is independent of indenting load. A possible interpretation of such a dependence can be envisaged in terms of the volume of a material that is sampled by the indenter. In other words, applying larger loads increases the volume that is tested and thus changes the effective resolution of the technique. It is the decrease in resolution with increasing load on the indenter that is believed to be responsible for the change in peak hardness with load as seen in Fig. 3. In other words, the smaller

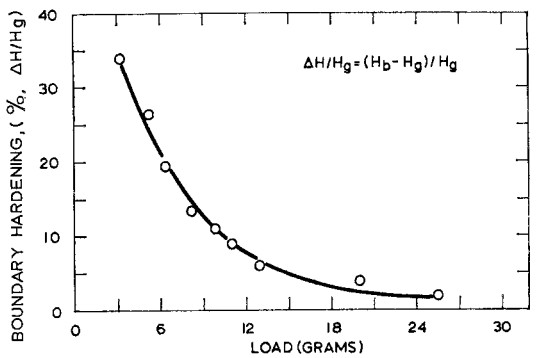

Figure 3 Variation of the grain-boundary hardness increment with load.

the indenting load, the smaller will be the difference between the apparent (measured) and the true hardness/distance dependence in the vicinity of a grain boundary. On the other hand, the constancy of the width of the hardened region around the boundary for different indenting loads (Fig. 2) indicates that a change in the volume which is tested (resolution of the technique) for the range of loads used does not affect the width of the apparent zone of hardening, found to extend ~ 40 μm on either side of the boundary [12]. Hence, it is believed that this is the extent of the true hardening.

4.2. Zone of deformation around the indentation

In view of the above results, it was considered

interesting to determine the extent of the deformed zone associated with a micro-indentation. The plastic component of this zone, i.e. the work-hardened region around the indentation, is rather simple to determine as it is associated with the plastic deformation that remains permanently in the material upon removal of the indenter. The extent of this zone of plastic deformation was determined by traversing the vicinity of several big indentations made by loads ranging from 10 to 30 g with a load of 3.3 g. Because of the grain-boundary hardening effect, all the big indentations were located in the centres of the grains; the grain size of the specimen used was 500 μm. The distances between the centres of the indentations were measured and the hardness/distance profiles of the work-hardened zone for each load used were obtained. As an illustration, Fig. 4 shows hardness/distance profiles for loads of 10, 20 and 30 g. From this figure, it is clear that the hardness in the vicinity of the impressions decreases rapidly with increasing distance from the centres of these indentations and levels off with the bulk hardness at some critical distance. In Fig. 5 are shown the same data for the hardness/distance profiles but as a function of the ratio r/h_o, where r is the distance between the centres of the indentations and h_o is the depth of penetration during loading (see Fig. 1) calculated from measured diagonals and known geometry of the indenter, for the loads used, bearing in mind the fact that diagonals are not affected by the elastic recovery that indentations undergo after removal of the indenting load.

From this figure, it is clear that all the data fall

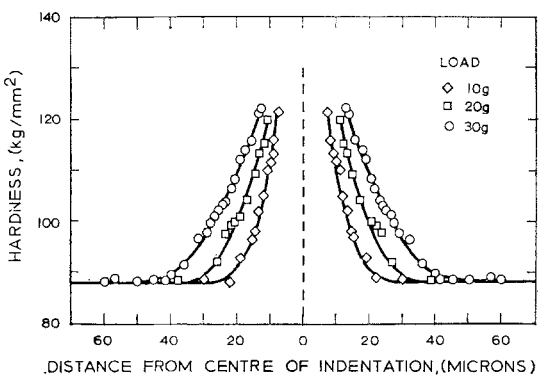

Figure 4 Hardness/distance profile near the big indentations obtained by traversing the vicinity of these indentations by the load 3.3 g.

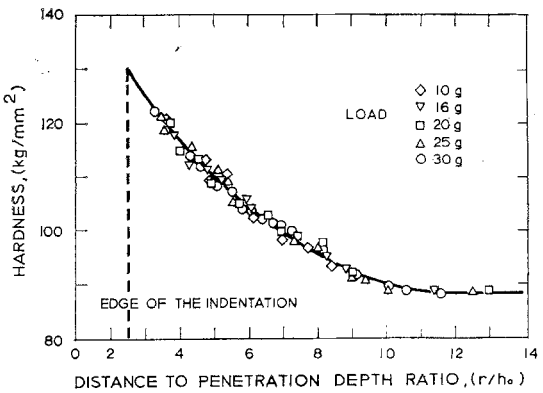

Figure 5 Variation of hardness near the big indentations with the ratio r/h_o.

on one master curve, and hardness gradually decreases with increasing r/h_o, finally levelling off at some critical value of this ratio; this value appears to be 10. In other words, the distance to which a work-hardened region extends is $\sim$ 10 times the depth of the indenter penetration. This is consistent with values previously reported in the literature [6, 7].

4.3. Elastic recovery of the indentations

The extent of elastic deformation around the indentation or the elastic component of the deformed zone is rather difficult to determine. Nevertheless, some insight into the order of magnitude of this deformation can be gained by determining the elastic recovery that the indentation undergoes after removal of the indenter.

Bearing in mind the fact that recovery of the indenter diagonal is negligible, that is to say $d_p \approx d_o$, it follows from Fig. 1 that the depth h_p that remains in the material is given as

$$h_p = \frac{d_o}{2\sqrt{2}} \tan' \alpha_p \qquad (5)$$

where α_p is the wedge angle that remains after removal of the indenter. This angle was determined interferentially using the Zeiss Interference Microscope and a modified formula due to Mykura [13].

$$\sin 2\alpha_p = \frac{\lambda}{\chi} \qquad (6)$$

where λ is the wavelength of the light used ($\lambda = 0.54$ μm) and χ is the spacing between fringes measured from the interferograms, such

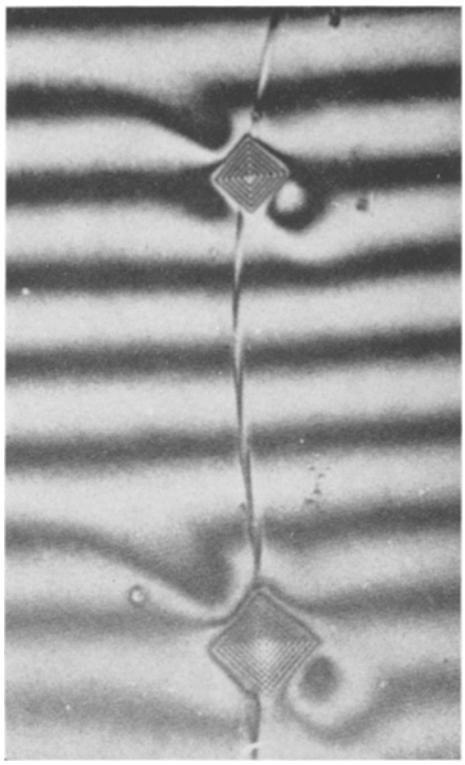

Figure 6 Interferogram of the micro-indentation located at grain boundary (× 350).

as shown on Fig. 6. This modified formula had to be used since the usual formula

$$h_p = m\frac{\lambda}{2} \tag{7}$$

is valid only for small wedge angles [13, 14]. The fractional error involved in using Equation 5 to determine the depth h_p is approximately $0.1/n$ where n is the number of fringes observed [13].

The elastic component of the depression, i.e. the elastic recovery in the direction of depth of penetration (h_e), was obtained as a difference

$$h_e = h_o - h_p \tag{8}$$

and with the calculated errors is shown in Fig. 7 as a function of applied load. From this figure, it is apparent that elastic recovery, h_e, increases with increasing the load on the indenter. It also appears that the recovery of an indentation located in a grain is greater than that of one located at a grain boundary, where smaller loads are used. For higher loads applied on the indenter, elastic recovery of a boundary indentation approaches that of a grain indentation. This dependence of elastic recovery is even better

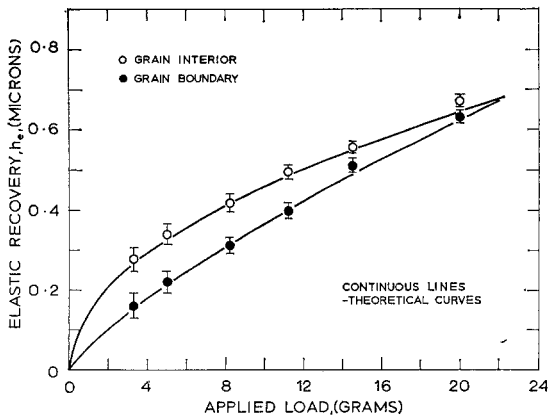

Figure 7 Variation of the elastic recovery of the micro-indentations in the direction of depth of the indenter penetration with load for the micro-indentations located at grain boundary and grain interior.

illustrated in Fig. 8, which shows elastic recovery of indentations defined as h_e/h_o in per cent, as a function of load. It is clear that the elastic recovery of indentations located in the grain interior shows a slight decrease while that of indentations at the grain boundaries shows an increase with increasing indenting load. For loads above 20 g the recovery of the boundary indentations attains the value of that of the bulk indentations, ~ 22%, and is apparently independent of further increase in load. This value for the recovery compares well with values previously reported in the literature for the elastic recovery of micro-indentations in iron [6].

It should be emphasized, however, that this high value for elastic recovery of micro-indentations defined as per cent h_e/h_o, does not correspond to the elastic strain limit of iron, generally accepted as ~ 0.1%. On the other

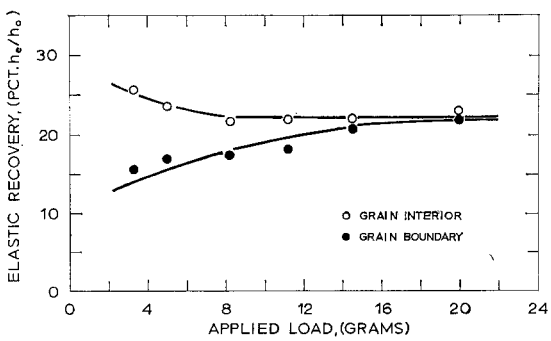

Figure 8 Variation of the elastic recovery defined as percentage of h_e/h_o of the micro-indentations located at grain boundary and bulk of the material.

hand, since the elastic recovery of indentations depends upon Young's modulus, an interpretation in terms of the difference betweent the elastic modulus of the boundary region and that of the bulk of the crystal would seem feasible.

In order to derive the elastic modulus and, also, to establish whether Love's analysis is applicable in the case of the diamond pyramid indenter, we shall assume, to a first approximation, that a pyramidal indentation is identical to a conical indentation. This assumption is fairly reasonable since tne deformation patterns and the extents of the deformed zones associated with conical and pyramidal indentations having the same apical angle, 138°, are identical [4]. Thus, using Equation 4 and inserting the values for υ and E for iron, i.e. $\upsilon = 0.28$ and $E = 20 \times 10^3$ kg/mm^2 [15], the elastic recovery $h_e{}^G$ for micro-indentations located in the centres of the grains can be calculated. The calculated values of $h_e{}^G$ are shown in Fig. 7 as a continuous line. Both the general trend and the actual values of the calculated curve compare well with the experimentally determined points. This good agreement between the calculated and experimental values enables the use of the same equation to calculate the values of the apparent elastic modulus E_G, using the experimentally determined values of $h_e{}^G$, provided it is assumed that the value for the Poisson's ratio remains the same, i.e. $\upsilon = 0.28$. The calculated best value for the apparent Young modulus of the bulk of the material is found to be $E_G = 19.5 \times 10^3$ kg/mm^2.

In view of these considerations, and from Fig. 7, it would appear that the elastic recovery of indentations located at grain boundaries, in the load range < 25 g, may be expressed by an equation similar to Equation 4, i.e.:

$$h_e{}^B = \left(\frac{\pi}{2}\cot\frac{\theta}{2}\right)^n \cdot \left(\frac{1-\upsilon_B{}^2}{E_B}\right)^n \cdot L^n \qquad (9)$$

where $n \neq \frac{1}{2}$, and υ_B and E_B are the Poisson's ratio and the Young's modulus describing the elastic properties of the grain-boundary "material". The exponent n can be determined from a linear plot of $\log h_e{}^B$ versus $\log L$ using the experimental points, and is found to be 0.77. By inserting this value in Equation 9 and taking $\upsilon_B = 0.28$, one can calculate E_B using the experimentally obtained values for the elastic recovery of micro-indentations located at grain boundaries ($h_e{}^B$). The value of elastic modulus, E_B, calculated in this way is found to be 15×10^3 kg/mm^2, and is independent of load in the load range considered. Equation 9 with inserted values for E_B, υ_B and n is also shown on Fig. 7 as a continuous line; it is clear that there is a good fit.

It should be pointed out that the approach described above would not be invalidated even if a different value for υ_B were taken. Calculations have shown that using values between 0.25 and 0.45, generally regarded as the range for Poisson's ratio for metals [16], does not alter significantly either the general trend of Equation 8 or the calculated values for E_B and $h_e{}^B$.

5. Discussion

The experimental results have unambiguously established that there is a difference in the behaviour of the micro-indentations located at grain boundaries compared with the behaviour of those located in the bulk of the material. The elastic recovery that these indentations undergo following removal of the indenter, is found to take place almost entirely in the direction of the depth whereas the contraction of the diagonals is practically negligible. The amount of contraction in the direction of depth (h_e) is load dependent; in the low load range (< 25 g), this contraction is larger for the bulk indentations than for those located at the grain boundaries. For loads above 25 g, there is no difference in the amount of contraction for bulk and boundary indentations.

This load dependence is consistent with the grain-boundary hardening which is found to diminish as the load on the indenter is increased. This can be explained in terms of the poor resolution of the micro-indentation technique when higher loads are applied. In other words, when the higher loads are applied, the indenter samples, not only the boundary material but also the bulk of the crystal. In such a case, the contribution of the former to the elastic recovery becomes negligible in comparison with the latter, since the greater part of the volume sampled by the indenter is comprised of the bulk material. Thus, whatever the cause for the behaviour of grain-boundary micro-indentations at lower loads, it is clear that it is averaged out when higher loads are applied.

The disappearance of boundary-hardening with increasing load is also consistent with the disappearance of the diversity in the elastic recovery behaviour of the micro-indentations located at grain boundaries and in the bulk of the material. Such a good correlation between these two effects implies that they are not due to the

intrinsic nature of the micro-indentation testing but are rather a measure of a property of grain boundaries throughout the crystal.

Further confirmation that such inhomogeneities are present in polycrystalline specimens come from a strong grain-boundary contribution to electrical resistivity. It has been shown that the observed variation of resistivity with grain size can be explained in terms of a narrow grain-boundary layer of higher resistivity than the remainder of the crystal [17].

Hence, it is believed that both effects, i.e. grain-boundary hardening and the difference in the elastic recovery, are associated with the presence of a narrow band of material around the boundary that is harder and has different elastic properties. Introduction of the elastic modulus concept to account for the local relation between stress (load) and strain emphasizes the difference in behaviour of the grain boundaries and the bulk of the material when small forces (loads up to 25 g) are applied on the indenter. However, this tentative, and in some cases very successful way of interpreting the results on grain-boundary hardening, in no way implies that the observed grain-boundary hardening can be entirely explained in terms of the change of the elastic properties. Furthermore, the real difficulty (and danger) in using the approach freely lies in the fact that some of the premises on which it is based are approximations rather than precise definitions with unambiguous meaning. Nevertheless, whatever the detailed mechanism of the grain-boundary hardening may be, it is clear that it also affects the elastic properties of the material near and at the grain boundary.

Finally, application of Love's over-simplified analysis of elastic deformation shows that there is a very good agreement between experimental and theoretical predictions, suggesting that the basic model is reasonably valid and that it may satisfactorily be applied.

Acknowledgement

The authors are indebted to Professor A. G. Quarrell for the provision of laboratory facilities at Sheffield. One of us (M.B.) is grateful to the Worshipful Company of Ironmongers for the provision of a financial support. Dr Edna Dancy of Hydro-Quebec Research Institute read the manuscript and made valuable comments.

References

1. J. H. WESTBROOK, *Met. Rev.* (London) **9** (1964) 415.
2. K. T. AUST, A. J. PEAT, and J. H. WESTBROOK, *Acta Metallurgica* **14** (1966) 1469.
3. M. BRAUNOVIĆ, C. W. HAWORTH, and R. T. WEINER, *Metal. Sci. J.* **2** (1968) 67.
4. A. G. ATKINS, A. SILVÉRIO, and D. TABOR, *J. Inst. Metals*, **94** (1966) 369.
5. T. O. MULHEARN, *J. Mech. Phys. Solids* **7** (1959) 85.
6. H. BÜCKLE, *Met. Rev.* (London) **4** (1959) 49.
7. L. E. SAMUELS and T. O. MULHEARN, *J. Phys. Mech. Solids* **5** (1957) 125.
8. N. A. STILWELL and D. TABOR, *Proc. Phys. Soc.* **78** (1961) 169.
9. A. E. H. LOVE, *Quart. J. Math.* **19** (1939) 161.
10. M. BRAUNOVIĆ and C. W. HAWORTH, *Metal Sci. J.* **4** (1970) 85.
11. *Idem, Prakt. Metallographie* **7** (1970) 183.
12. *Idem*, unpublished research.
13. H. MYKURA, *Proc. Phys. Soc.* (B) **67** (1954) 281.
14. W. KRUG, J. RENITZ, and G. SCHULTZ, "Beitrage zur Interfernzmikroskopie 1 Auflage (Akademie-Verlag, Berlin, 1961) p. 61.
15. W. J. MCGREGOR TEGART, "Elements of Mechanical Metallurgy" McMillan Series in Material Sciences (1966).
16. W. KOSTER and H. FRANTZ, *Met. Rev.* (London) **6** (1961) 1.
17. M. BRAUNOVIĆ and C. W. HAWORTH, *J. Appl. Phys.* **40** (1969) 3459.

Received 17 January and accepted 26 January 1972.